Projection Algorithms for Phase Retrieval with High Numerical Aperture

Presenter: Nguyen Hieu Thao

DCSC
Delft Center for Systems and Control

Variational Analysis and Optimisation Seminar, August 19, 2020

Outline

Phase retrieval

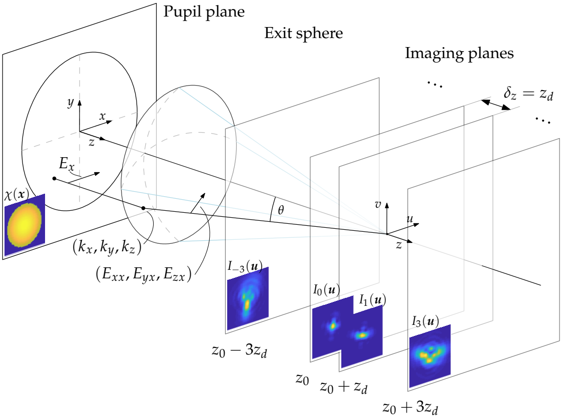

Figure: [1] Schematic diagram of phase retrieval given several PSF images.

[1] N. H. Thao, O. Soloviev and M. Verhaegen, *Phase retrieval based on the vectorial model of point spread function*. JOSA A **37**, 16–26, 2020.

Outline

Light as an electromagnetic radiation

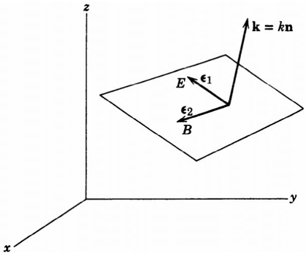

Figure: [2] Propagation vector **k** and two orthogonal polarization vectors.

- transverse, plane wave (frequency ω, direction $\mathbf{k}$)
- spatially constant permeability and susceptibility
- harmonic time dependence $\mathrm{e}^{-\mathrm{j}\omega\mathrm{t}}$
- the Helmholtz wave equation & the Maxwell equations

The electric field

$$E(\mathbf{x}, t) = (\epsilon_1 E_1 + \epsilon_2 E_2)\, \mathrm{e}^{\mathrm{j}\mathbf{k}.\mathbf{x} - \mathrm{j}\omega\mathrm{t}}$$

[2] J. D. Jackson, *Classical Electromagnetic*, *3rd edition*. John Wiley & Sons, 1999.

Linear polarization

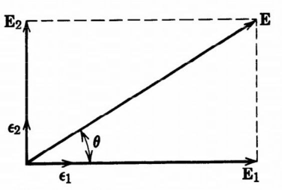

Figure: [3] Electric field of linearly polarized wave.

E_1, E_2 have the same phase $\Longleftrightarrow$ linear polarization

$$E(\mathbf{x}) = \epsilon_1 E_1 + \epsilon_2 E_2 = \epsilon\,\chi(\mathbf{x})\,\mathrm{e}^{\mathrm{j}\Phi(\mathbf{x})}$$

Generalized pupil function $\quad G(\mathbf{x}) = \chi(\mathbf{x})\,\mathrm{e}^{\mathrm{j}\Phi(\mathbf{x})}$

[3] J. D. Jackson, *Classical Electromagnetic*, *3rd edition*. John Wiley & Sons, 1999.

Bending of the polarization vector

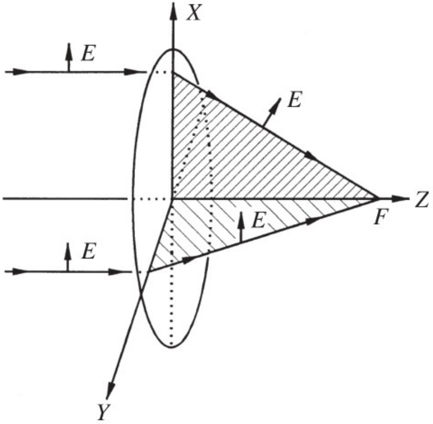

Figure: [4] The polarization vector changes after the lens.

[4] M. Mansuripur, *Classical Optics and its Applications*, *2nd edition*. Cambridge University Press, 2009.

Scalar point-spread-function (PSF)

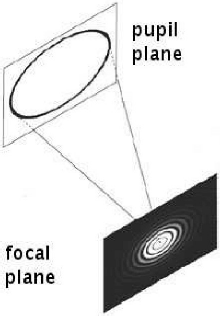

Figure: [5] The GPF is related to PSFs via the Fourier transform.[6]

Scalar PSF ignores the change of polarization direction.

$$p_s(\mathbf{u}) = \left|\mathcal{F}\{G(\mathbf{x})\}\right|^2$$

[5] M. Verhaegen, G. Vdovin and O. Soloviev, *Control for High Resolution Imaging*, *Lecture Notes*. Delft University of Technology, 2015.

[6] J.W. Goodman, *Introduction to Fourier Optics*, *5th edition*. Roberts & Company Publishers, 2017.

Bending of polarization vector

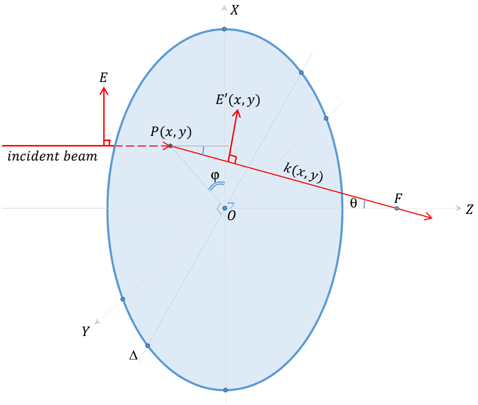

Figure: [7] The amount of bending depends on the ray's coordinates.

$$E' = \mathcal{R}^{-1}_{(OZ,\varphi)} \circ \mathcal{R}_{(OY,\theta)} \circ \mathcal{R}_{(OZ,\varphi)}(E)$$

[7] N.H. Thao, O. Soloviev, D.R. Luke and M. Verhaegen, *Projection methods for high numerical aperture phase retrieval*. Manuscript in preparation.

Bending of $E_x(1,0,0)$ and $E_y(0,1,0)$

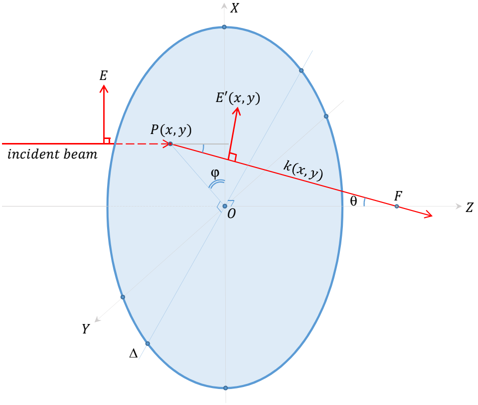

$$E_{xx} = 1 - k_x^2/(1+k_z)\,; \quad E_{yx} = -k_x k_y/(1+k_z)\,; \quad E_{zx} = -k_x$$

$$E_{xy} = -k_y k_x/(1+k_z)\,; \quad E_{yy} = 1 - k_y^2/(1+k_z)\,; \quad E_{zy} = -k_y$$

Aperture normalization: $k_x^2 + k_y^2 \leq \mathrm{NA}^2$

TUDelft

Vectorial PSF - known polarization direction

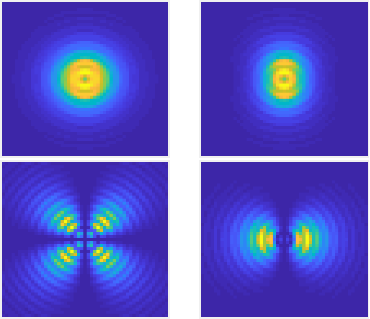

Vectorial PSF with vertical polarization direction & its components.

$$p_{E_x}(\mathbf{u}) = \left|\mathcal{F}\{E_{xx} \cdot G(\mathbf{x})\}\right|^2 + \left|\mathcal{F}\{E_{yx} \cdot G(\mathbf{x})\}\right|^2 + \left|\mathcal{F}\{E_{zx} \cdot G(\mathbf{x})\}\right|^2$$

Modified GPF [8] $\quad G(x) \longrightarrow k_z^{-1/2} \cdot G(x)$

[8] M. Mansuripur, *Classical Optics and its Applications*, *2nd edition*. Cambridge University Press, 2009.

Vectorial PSF - unknown polarization direction

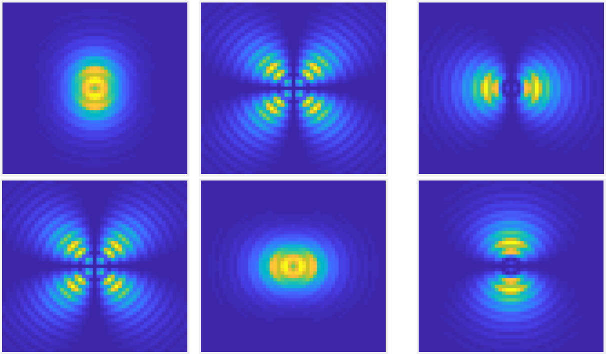

Components of vectorial PSF with random polarization direction.[9]

$$p(\mathbf{u}) = \sum_{cc \in \mathcal{I}} \left|\mathcal{F}\{E_{cc} \cdot G(\mathbf{x})\}\right|^2, \; \mathcal{I} = \{xx, yx, zx, xy, yy, zy\}$$

[9] M. Mansuripur, *Classical Optics and its Applications*, *2nd edition*. Cambridge University Press, 2009.

When vectorial PSFs needed?

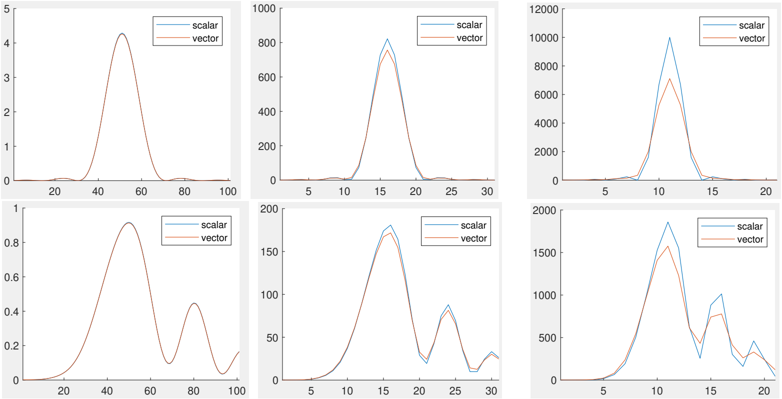

Comparison between scalar & vectorial PSFs for various NA values.

Outline

PR given multiple PSF images

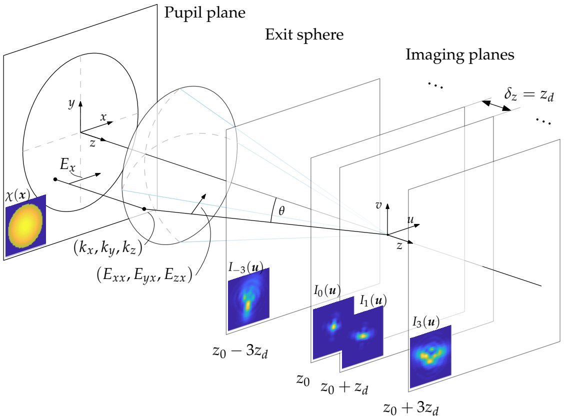

$$I_d = \sum_{cc \in \mathcal{I}} \left| \mathcal{F}\left(E_{cc} \cdot \chi \cdot e^{j(\Phi + \phi_d)} \right) \right|^2 + \omega_d, \quad (d = 1, \ldots, m)$$

Out-of-focus PSF $\implies \phi_d = \frac{2\pi}{\lambda} z_d \sqrt{1 - k_x^2 - k_y^2}$

The ambient space and constraints

$$\mathcal{H} = \underbrace{\mathbb{C}^{n\times n} \times \mathbb{C}^{n\times n} \times \cdots \times \mathbb{C}^{n\times n}}_{\text{6 times}}$$

- General constraint

$$\Omega_0 = \left\{ \left(E_{cc} \cdot x \right)_{cc \in \mathcal{I}} \in \mathcal{H} \;\middle|\; x \in \mathbb{C}^{n\times n} \right\}$$

- Intensity constraint $(d = 1, \ldots, m)$

$$\Omega_d = \left\{ \left(u_{cc} \right)_{cc \in \mathcal{I}} \in \mathcal{H} \;\middle|\; \sum_{cc \in \mathcal{I}} \left| \mathcal{F}\left(E_{cc} \cdot u_{cc} \cdot \mathrm{e}^{\mathrm{j}\phi_\mathrm{d}} \right) \right|^2 = I_d \right\}$$

- Amplitude constraint

$$\Omega_\chi = \left\{ \left(E_{cc} \cdot \chi \cdot \mathrm{e}^{\mathrm{j}\Phi} \right)_{cc \in \mathcal{I}} \in \mathcal{H} \mid \Phi \in \mathbb{R}^{n\times n} \right\}$$

A feasibility model (nonconvex!)

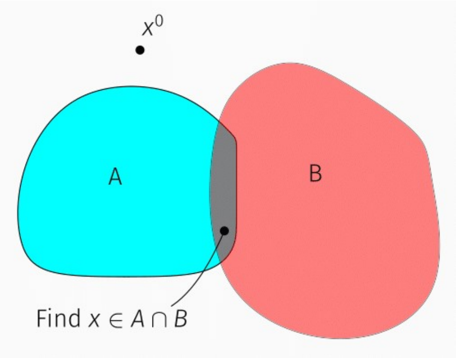

$$A \equiv \{(u, \ldots, u) \in \mathcal{H}^m \mid u \in \Omega_0\}, \; B \equiv \Omega_1 \times \cdots \times \Omega_m;$$

Known amplitude $\implies$ Ω_0 is replaced by Ω_χ

Outline

Projection operators (I)

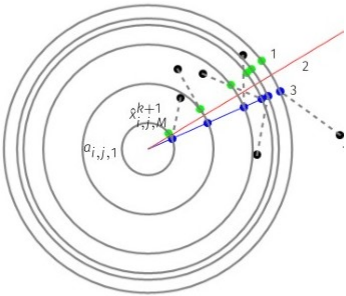

Figure: Projector on $\Omega_0 \equiv \{(E_{cc} \cdot x)_{cc \in \mathcal{I}} \in \mathcal{H} \mid x \in \mathbb{C}^{n \times n}\}$.

$$(u \in \mathcal{H}) \quad P_{\Omega_0}(u) = \left\{\left(E_{cc} \cdot a \cdot \mathrm{e}^{\mathrm{j}\Psi}\right)_{cc \in \mathcal{I}}\right\}$$

$$\text{where} \quad \Psi \in \arg\left(\sum_{cc \in \mathcal{I}} (E_{cc} \cdot u_{cc})\right), \; a = \frac{1}{2}\left|\sum_{cc \in \mathcal{I}} (E_{cc} \cdot u_{cc})\right|$$

Projection operators (II)

Feasibility formulation: find $x \in A \cap B \subset \mathcal{H}^m$

[10] For $x = (x_1, \ldots, x_m) \in \mathcal{H}^m$,

- $P_A(x) = \underbrace{P_{\Omega_0}(\overline{x}) \times \cdots \times P_{\Omega_0}(\overline{x})}_{m \text{ times}}$ where $\overline{x} = \frac{1}{m}\sum_{d=1}^m x_d$
- $P_B(x) = P_{\Omega_1}(x_1) \times \cdots \times P_{\Omega_m}(x_m)$

Known amplitude $\Longrightarrow$ Ω_0 is replaced by Ω_χ

[10] N.H. Thao, O. Soloviev, D.R. Luke and M. Verhaegen, *Projection methods for high numerical aperture phase retrieval*. Manuscript in preparation.

Examples of projection methods

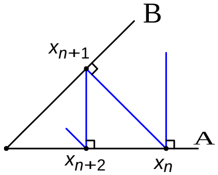

- AP method (the figure): $T_{AP} = P_A P_B$
- DR algorithm: $T_{DR} = \frac{1}{2}(R_A R_B + \mathrm{Id})$, where $R_A = 2P_A - \mathrm{Id}$
- [11] HIO method: $T_{HIO} = P_A((1+\beta)P_B - \mathrm{Id}) - (\beta P_B - \mathrm{Id})$
- [12] RAAR algorithm: $T_{RAAR} = \beta T_{DR} + (1-\beta)P_B$
- [13] DRAP algorithm: $T_{DRAP} = \beta T_{DR} + (1-\beta)T_{AP}$

[11] J.R. Fienup, *Phase retrieval algorithms: a comparison*. Appl. Opt. **21** (1982).

[12] D.R. Luke, *Relaxed averaged alternating reflections for diffraction imaging* Inverse Problems **21** (2005).

[13] N.H. Thao, *A convergent relaxation of the Douglas-Rachford algorithm*. Comput. Optim. Appl. **70** (2018).

Outline

TUDelft

Analysis scheme [14]

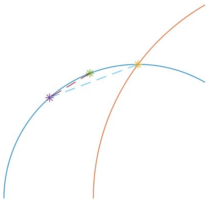

Figure: Picard iterations progress not too slowly by metric regularity.

a T almost α-averaged at $\bar{x} \in \operatorname{Fix} T$ on U:

$$\|x^+ - \bar{x}\|^2 \le (1+\varepsilon)\|x - \bar{x}\|^2 - \frac{1-\alpha}{\alpha}\|x - x^+\|^2, \quad \forall x \in U, x^+ \in T(x)$$

b Metric regularity condition: $\exists \kappa < \sqrt{(1-\alpha)/\varepsilon\alpha}$ s.t.

$$\operatorname{dist}(x, \operatorname{Fix} T) \le \kappa \|x - x^+\|, \quad \forall x \in U, x^+ \in T(x)$$

Then $\forall x_0 \in U$, $T^k(x_0)$ converges linearly to $\operatorname{Fix} T$.

[14] D.R. Luke, N.H. Thao and M.K. Tam, *Quantitative convergence analysis of iterated expansive, set-valued mappings*. Math. Oper. Res. **43**, 1143–1176 (2018).

TUDelft

Geometry of high-NA phase retrieval

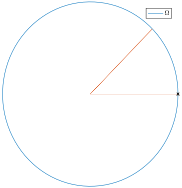

Figure: Circles are typical example of prox-regularity.

Ω prox-regular at $\bar{x} \iff P_\Omega$ single-valued around $\bar{x}$

Projector on $\Omega_0 = \{(E_{cc} \cdot u)_{cc \in \mathcal{I}} \in \mathcal{H} \mid u \in \mathbb{C}^{n \times n}\}$ is

$$P_{\Omega_0}(u) = \left\{\left(E_{cc} \cdot a \cdot \mathrm{e}^{\mathrm{j}\Psi}\right)_{cc \in \mathcal{I}}\right\}$$

where $\Psi \in \arg\left(\sum_{cc \in \mathcal{I}} (E_{cc} \cdot u_{cc})\right)$, $a = \frac{1}{2}\left|\sum_{cc \in \mathcal{I}} (E_{cc} \cdot u_{cc})\right|$

Equivalent to the geometry of low-NA phase retrieval

Convergence of AP

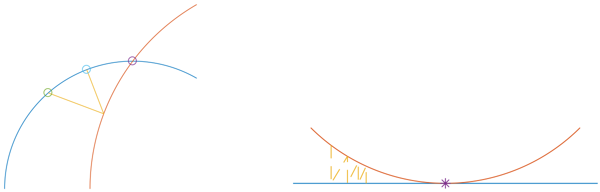

Figure: Subtransversality (left) versus tangency (right)

- (a) Almost averagedness $\longleftarrow$ geometry of PR
- (b) Metric regularity $\longleftarrow$ subtransversality of $\{A, B\}$ at $\bar{x}$

$$d(x, A \cap B) \leq \kappa \max\{d(x, A), d(x, B)\} \quad \forall x \text{ near } \bar{x}$$

$\Longrightarrow$ linear convergence [15]

[15] N.H. Thao, O. Soloviev, D.R. Luke and M. Verhaegen, *Projection methods for high numerical aperture phase retrieval*. Manuscript in preparation.

Outline

NA analysis

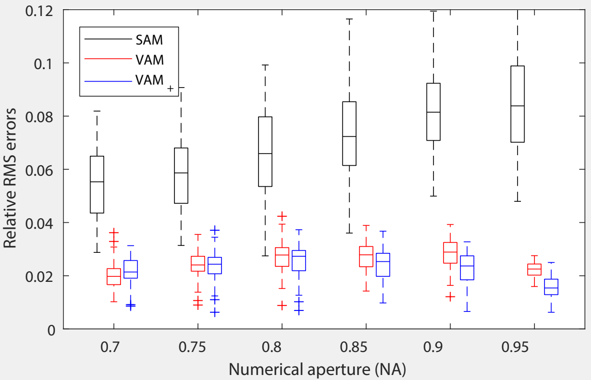

Vectorial PSF is more essential for higher NA value.

Noise analysis

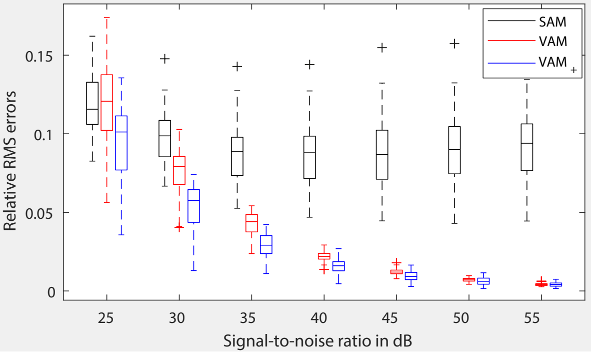

The advantage of the vectorial PSF reduces for more noise.

Convergence analysis

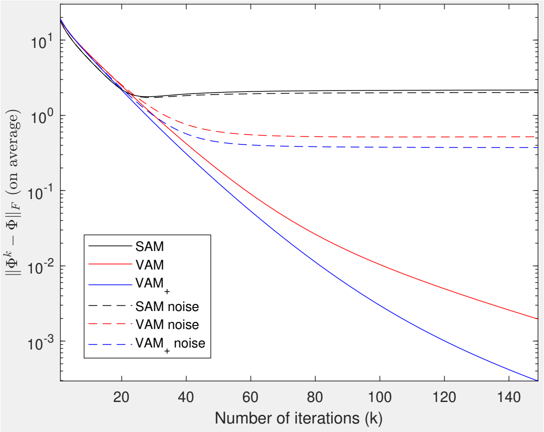

Linear convergence is consistently observable.

A realization of phase retrieval

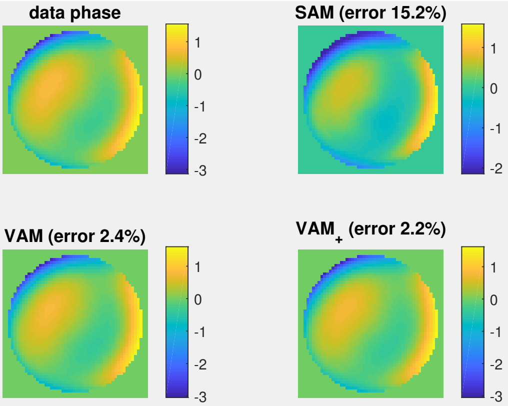

More accurate imaging model leads to more precise restoration.

Other projection algorithms

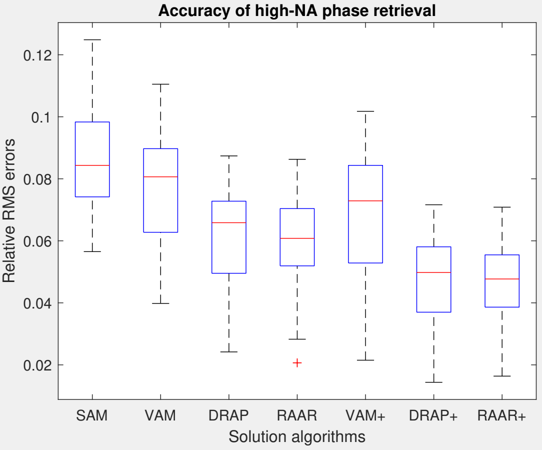

RAAR and DRAP yield more accurate restoration.

Concluding remarks

The class of projection algorithms is extended for high-NA PR.

- Rigorous mathematical explanation
- Closed forms of projectors
- Geometry of high-NA PR
- Convergence analysis (the level of low-NA PR)
- Numerical results (deliverable to our industrial customer)

Challenge: vectorial PSF is more sensitive to noise than the scalar.

Main References (I)

- J.W. Goodman, *Introduction to Fourier Optics*, *5th edition*. Roberts & Company Publishers, 2017.
- J.D. Jackson, *Classical Electromagnetic*, *3rd edition*. John Wiley & Sons, 1999.
- M. Mansuripur, *Classical Optics and its Applications*, *2nd edition*. Cambridge University Press, 2009.
- M. Verhaegen, G. Vdovin and O. Soloviev, *Control for High Resolution Imaging*, *Lecture notes*. TU Delft, 2015.
- N.H. Thao, O. Soloviev and M. Verhaegen, *Phase retrieval based on the vectorial model of point spread function*. JOSA A **37**, 2020.

Main References (II)

- N.H. Thao, O. Soloviev, D.R. Luke and M. Verhaegen, *Projection methods for high numerical aperture phase retrieval*. Manuscript in preparation.
- J.R. Fienup, *Phase retrieval algorithms: a comparison*. Appl. Opt. **21**, 1982.
- D.R. Luke, *Relaxed averaged alternating reflections for diffraction imaging*. Inverse Problems **21**, 2005.
- D.R. Luke, N.H. Thao and M.K. Tam, *Quantitative convergence analysis of iterated expansive, set-valued mappings*. Math. Oper. Res. **43**, 2018.
- N.H. Thao, *A convergent relaxation of the Douglas–Rachford algorithm*. *Comput. Optim. Appl.* **70**, 2018.

WITH THANKS TO

MADEin4

ECSEL Joint Undertaking
Electronic Components and Systems for European Leadership

This project has received funding from the ECSEL Joint Undertaking (JU) under grant agreement No. 826589. The JU receives support from the European Union's Horizon 2020 research and innovation programme and Netherlands, Belgium, Germany, France, Italy, Austria, Hungary, Romania, Sweden and Israel.

TU Delft Delft University of Technology